Eur. J. Wood Prod. (2014) 72:331–341
DOI 10.1007/s00107-014-0781-0

ORIGINAL

Model for the prediction of the tensile strength and tensile stiffness of knot clusters within structural timber

Gerhard Fink · Jochen Kohler

Received: 18 December 2012 / Published online: 22 February 2014

Abstract In the present paper, a model for the prediction of the local strength and stiffness properties is developed. Compared to existing models, here the local material properties are described according to their morphological characteristics; i.e. the timber boards are subdivided into sections containing knots (knot sections) and sections without knots (clear wood sections). The strains of the corresponding sections are measured during non-destructive tensile tests using an optical camera device. Based on these measurements the tensile stiffness of each particular section is estimated. For the estimation of the tensile strength, destructive tensile tests are performed. Herewith, the tensile strength of the entire timber board is measured. The strength of the other knot clusters are estimated using censored regression analysis. Taking into account the results of the experimental investigation, material models are developed to predict the tensile strength and the tensile stiffness of knot clusters.

1 Introduction

Timber is a natural grown material which has, compared to other building materials, a large variation in its load-bearing behaviour. This variation can be observed between different growth regions, between different boards within the same growth region and even within one particular timber board (e.g. Fewell 1982; Köhler et al. 2007; Sandomeer et al. 2008). As a simplification, the variation can be subdivided into (a) the variation between the timber boards and (b) the variation within the timber boards. In the past, numerous models have been developed to describe the variability of the material properties; e.g. Isaksson (1999) for ultimate bending capacity, Taylor and Bender (1991) and Kohler et al. (2013) for ultimate tensile capacity and bending stiffness, Kline el al. (1986) for bending stiffness and Fink and Kohler (2011) for tensile stiffness.

The variability between the timber boards or rather the variability of the undisturbed timber (knot free timber—denoted as clear wood) is related to different growth and sawing characteristics; e.g. growth region, sapwood-heartwood. For the predictions of the mean material properties, different non-destructive test methods have been developed in the last decades. The most common methods are the Eigenfrequency measurement (e.g. Kollmann and Krech 1960; Görlacher 1990), the Ultrasonic runtime measurement (Steiger 1996) and the density. In several studies, correlations between those parameters and the material properties are analysed (e.g. Görlacher 1984; Steiger 1996; Denzler 2007). In particular the first two methods, which are Eigenfrequency and ultrasonic runtime, show an exceptionally good correlation to the mean material properties.

The variability of the strength and stiffness properties within structural timber is highly dependent on morphological characteristics of the tree, especially it is dependent on knots and their arrangement. Accordingly, numerous studies have been conducted to identify knot related indicators that are capable of describing the influence of knots on the load-bearing behaviour of timber boards relevant for the design of timber structures. Various models that represent the interrelation between numeral knot indicators

G. Fink (✉)
Institute of Structural Engineering, ETH Zurich,
Stefano-Franscini-Platz 5, 8093 Zurich, Switzerland
e-mail: fink@ibk.baug.ethz.ch

J. Kohler
Department of Structural Engineering, NTNU Trondheim,
Rich. Birkelandsvei 1A, 7491 Trondheim, Norway

and the load-bearing capacity exist. E.g. Denzler (2007), Isaksson (1999), Boatright and Garrett (1979a; 1979b), Courchene et al. (1996), Mitsuhashi et al. (2008) and Fink et al. (2011) have analysed the interrelation between ultimate bending and/or tensile capacity for different knot indicators. Mention that many times the load-bearing capacity of the weakest section (e.g. the knot cluster with the highest tKAR-value) is assumed as the load-bearing capacity of the entire timber board. The interrelation between the stiffness properties and knot indicators are analysed in Samson and Blanchet (1992) and Fink et al. (2011). In all studies described above, no knot-indicator could be found for an efficient prediction of the strength and stiffness properties of structural timber without considering additional indicators, such as the density. However, the so called tKAR-value (total knot area ratio) is established as one of the most efficient.

Regarding the between and within-member variability of the material properties it is obvious that an efficient model for the prediction of the local strength and stiffness properties should include at least two indicators: (a) one that describes the mean material properties of the entire timber board, to consider the between member-variability of the mean material properties, and (b) one that describes the local strength and stiffness reduction through the occurrence of knots and knot cluster, to consider the within-member variability. Such an approach has already been used within the model presented in Blaß et al. (2008). There, the material properties of 150 mm long board segments are predicted using the dry density ρ_0 and the tKAR-value based on material models developed by Glos (1978) and Ehlbeck et al. (1985), see also Heimeshoff and Glos (1980) for the test set-up. The models are developed based on material properties measured on specimens having a testing length of 137.5 mm.

In this paper, models for the prediction of the local material properties, based on experimental investigations of full scale timber boards (testing length >3,300 mm) are developed. Thereby it is particular focused on the prediction of the tensile strength and the tensile stiffness of knot clusters. Models to predict the following material properties are developed:

- Tensile stiffness of clear wood
- Tensile stiffness of knot clusters
- Tensile strength of timber boards
- Tensile strength of knot clusters

2 Experimental analysis

The experimental investigation includes the estimation of the tensile stiffness, the tensile strength and the dynamic modulus of elasticity as well as the measurement of all knots with a diameter larger than 10 mm. For the estimation of the tensile stiffness, non-destructive tensile tests are performed. The specific characteristic of this part of the experimental investigation is that the timber boards are previously subdivided into (a) sections containing knot clusters or large single knots (referred to as knot sections—KS), and (b) sections between the knot sections (referred to as clear wood sections—CWS). From all those sections the corresponding expansion is measured using an optical camera device.

2.1 Material

The stiffness properties are analysed based on two samples, each of 100 specimens; the species is Norway spruce (*Picea abies*) from Southern Germany. The boards are graded into the strength classes L25 and L40 according to the European standard EN 14081-4. The dimensions are 126 × 44 × 4,000 mm^3. According to EN 14081-4 the strength classes L25 and L40 require a minimum characteristic tension capacity of 14.5 and 26.0 MPa, respectively. The grading of the boards is performed by the GoldenEye-706 grading device manufactured by MiCROTEC (Brixen, IT) (Giudiceandrea 2005).

The tensile capacity is analysed individually for three samples, each of 150 randomly selected Swiss grown Norway spruce specimens. The dimensions of these reference samples are 90 × 45 × 4,000 mm^3, 110× 45× 4,000 mm^3, and 230 × 45 × 4,000 mm^3, respectively. The timber boards are randomly selected and not graded, thus their material properties should represent the basic population of Swiss grown Norway spruce.

In the following, the timber boards that are used to estimate the tensile stiffness are called Sample A, whereas the timber boards that are used to estimate the tensile strength are called Sample B.

For all timber boards, the dimensions and the position of every knot with a diameter larger than 10 mm are assessed and recorded. Furthermore, on Sample B destructive tensile tests are performed to estimate the ultimate tensile capacity and on Sample A non-destructive tensile tests are performed to estimate the tensile stiffness. In order to ensure comparability of the test results, all tension tests are performed with standard moisture content according to EN 408; i.e. equilibrium moisture content of the specimen in standard climate: (20 ± 2) °C and (65 ± 5) % relative humidity.

2.2 Non-destructive tensile tests

The stiffness properties are measured with an infrared camera device during non-destructive tensile tests. The

camera device, contains three interconnected cameras and the entire measured area (optical range of the infrared camera) is calibrated. The timber boards are subdivided into KS and CWS. At the beginning and the end of each section and at the edge of the total measured area, three high frequent infrared light emitting diodes (LEDs) are mounted (Figs. 1, 2). The boards are loaded with an axial tension force, which represents 45 % of the estimated maximum tensile capacity. The maximum tension capacity has been estimated based on the measurements of the GoldenEye-706 grading device. Over the entire time of the tensile test, the LEDs send light impulses with a frequency of 20 Hz and based on this their positions are measured with the infrared camera device. Each timber board is measured twice (at the top and bottom side).

For the estimation of the modulus of elasticity (denoted MOE), the strains over the board axis (calculated with the relative LED displacement of both sides) are used. The local strains within the KS are not considered separately. The assessment of the MOE is made by means of a linear regression model of the stress strain estimates according to

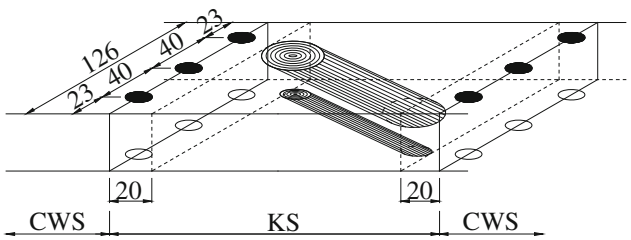

Fig. 1 LED-arrangement around a knot cluster

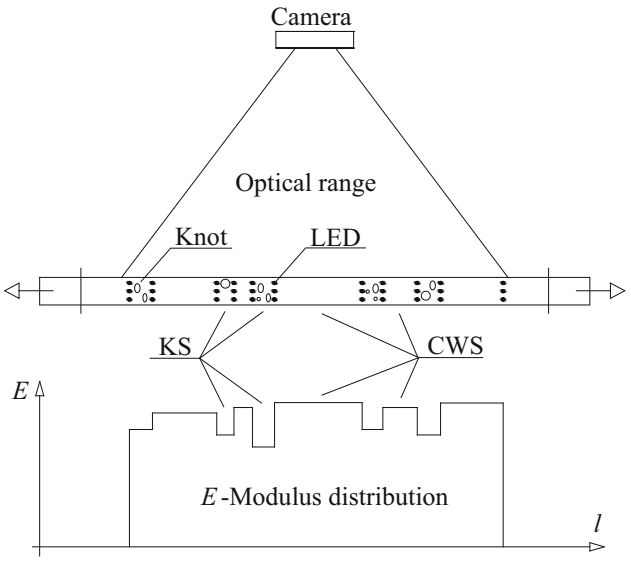

Fig. 2 Illustration of the experimental setup

EN 408; i.e. with strains between 10 and 40 % of the estimated maximum tensile capacity. However, it has to be noted that some configurations for the determination of the MOE do not completely conform to the requirements according to EN 408. According to EN 408, the calculation of the MOE by means of linear regression requires a coefficient of determination $R^2 \geq 0.99$ measured over a length of five times the width. For the investigated test specimens, this requirement would be equal to a range for the strain measurement of 630 mm. In the present study, the length is in general significantly shorter; e.g. the average length of KS being equal to 94 mm. Furthermore, the measured data show a random fluctuation (noise) by using this measurement device. As a result of the significantly reduced measurement length combined with the random fluctuation of the data, the requirements for the MOE estimation are reduced; i.e. the coefficient of determination $R^2 \geq 0.96$. The mean MOE over the total measured area is estimated based on the measured strain between the outmost LEDs.

The properties of the KS depend on parameters, such as size of the knots and/or the knot arrangement. Thus, the probabilistic characteristics of the properties of the KS are difficult to describe. Therefore, a weak section (WS) with a unit length $c = 150$ mm is introduced. The MOE of the KS is converted into the MOE of a WS according to Eq. (1). In this equation, the MOE of the WS $E_{j,WS}$ is calculated utilizing the estimated MOE of the corresponding KS $E_{j,KS}$, and the MOEs of the two adjacent CWS $E_{j-1,CWS}$ and $E_{j+1,CWS}$. $l_{j,KS}$ denotes the length of the corresponding KS (see also Fink and Kohler 2011).

$$\frac{1}{E_{j,WS}} = \frac{1}{c}\left(\frac{l_{j,KS}}{E_{j,KS}} + \frac{c - l_{j,KS}}{2E_{j-1,CWS}} + \frac{c - l_{j,KS}}{2E_{j+1,CWS}}\right) \quad \text{for} \quad l_{j,KS} \leq 150 \text{ mm}$$
$$E_{j,WS} = E_{j,KS} \quad \text{for} \quad l_{j,KS} \geq 150 \text{ mm} \tag{1}$$

In Fig. 3a, the estimated MOE of each section and the estimated mean MOE are illustrated for one timber board. For a more detailed description of the test procedure see Fink and Kohler (2012).

2.3 Destructive tensile tests

The reference boards were tested destructively in tension with the same tension machine as described in Chapter 2.2. The tests have been performed according to EN 408 which requires a testing range of at least nine times the width of the boards. In order to collect as much information as possible about the individual boards, the test range was maximized over the whole testable range of the boards just being limited by the clamping jaws of the tensile test

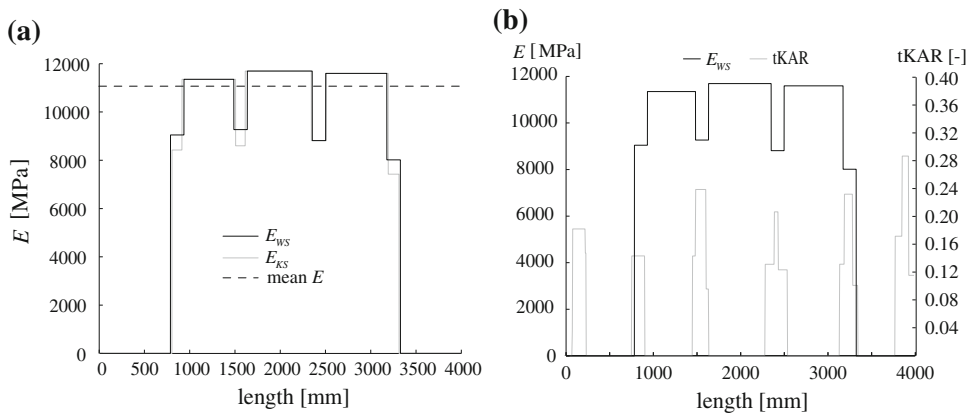

Fig. 3 **a** Example of the modulus of elasticity distribution, **b** illustration of the modulus of elasticity distribution and the corresponding tKAR-value

device at both ends of the timber boards. The resulting testing range corresponds to 3,360 mm.

2.4 Eigenfrequency measurement

For the prediction of the material properties of the undisturbed timber an Eigenfrequency measurement is performed on all specimens (Sample A + B). Therefore, in addition to the Eigenfrequency measurement f_0 the length l, the moisture content w, the density ρ (estimated through weight) and the dry density ρ_0 (estimated through w and weight) are measured. Based on the measurements the corresponding dynamic MOEs of each board $E_{\mathrm{dyn,F}}$ are calculated according to Eq. (2)—the Equation is developed based on the differential equation of the longitudinal stress waves in solids (see Kollmann and Krech 1960; Görlacher 1984 for a detailed description). The assessed values of the MOEs are corrected to a reference moisture content according to EN 384. The dynamic MOEs have to be considered as average values over the entire length of the timber board.

$$E_{\mathrm{dyn,F}} = (2lf_0)^2\rho \tag{2}$$

2.5 Knot measurement

To consider the within-member variability of the timber boards the knots are measured. Each knot with a diameter larger than 10 mm is assessed and recorded. Based on this the tKAR-value is calculated. This value is defined as the ratio between the projected knot area within a length of 150 mm and the cross sectional area (Isaksson 1999).

To show the influence of knots or rather the influence of the tKAR-value on the within-member variability, the estimated tensile stiffness and the corresponding tKAR-value of one specimen is illustrated in Fig. 3b. It is obvious that within the areas of the occurrence of knots the stiffness is significantly reduced.

3 Model to predict the tensile stiffness

As described above, timber shows a variability of its material properties, between and within the member. Therefore, it is obvious that an efficient model for the prediction of the local stiffness properties should include at least one indicator to consider the between-member variability, and one indicator to consider the within-member variability. To consider the between-member variability, the estimated dynamic MOE based on Eigenfrequency measurement $E_{\mathrm{dyn,F}}$ is used. For considering the within-member variability, the tKAR-value is chosen. In the following, two different models are developed. The first one can be used to predict the stiffness of the undisturbed timber, whereas the second one can be used to predict the local stiffness properties of a knot cluster.

For both cases, a linear regression model (Eq. 3) is used, where Y is the predicted stiffness, β_i are the regression coefficients, X are the input variables and ε is the error term. The input variable X_1 stands for $E_{\mathrm{dyn,\ F}}$ and the input variable X_2 stands for tKAR.

$$\ln(Y) = \beta_0 + \beta_1 X_1 + \beta_2 X_2 + \varepsilon \tag{3}$$

The parameters of the regression model and their uncertainties are estimated using maximum likelihood method; see e.g. Benjamin and Cornell (1970).

Based on the assumption of a normal distributed error term ε, the parameters of the regression model β_i and the standard deviation of the error term σ_ε, can be calculated as follows:

$$\boldsymbol{\beta} = (\hat{\boldsymbol{X}}^T\hat{\boldsymbol{X}})^{-1}\hat{\boldsymbol{X}}^T\hat{\boldsymbol{y}} \tag{4}$$

$$\sigma_\varepsilon^2 = \sqrt{\frac{\sum_{i=1}^{n}\varepsilon_i^2}{n-k}} \tag{5}$$

The uncertainties of the parameters β_i and σ_ε can be expressed with covariance matrix $C_{\Theta\Theta}$, where the diagonals are the variances of the parameters (β_i and σ_ε), and the other elements are the covariances between the

parameters. The covariance matrix $C_{\Theta\Theta}$ is defined as the inverse of the Fisher information matrix **H**. The components of **H** are determined by the second order partial derivatives of the log-likelihood function; see e.g. Faber (2012).

$$\mathbf{C}_{\Theta\Theta} = \mathbf{H}^{-1} \tag{6}$$

$$H_{ij} = -\frac{\partial^2 l(\boldsymbol{\theta}|\hat{\boldsymbol{x}})}{\partial\theta_i \partial\theta_j}|_{\boldsymbol{\theta}=\boldsymbol{\theta}^*} \tag{7}$$

3.1 Model to predict the stiffness of undisturbed timber

The first stiffness model is developed in order to predict the mean stiffness properties of defect-free timber within one timber board $E_{\overline{CWS}}$. Here $E_{\overline{CWS}}$ is calculated with the stiffness of all measured CWS within one board in accordance with Hook's law of serial springs (Eq. 8). In addition, a model for the prediction of the mean tensile stiffness of the entire timber board $\overline{E}$ is developed. For both models, only the first indicator $E_{\mathrm{dyn,F}}$ is taken into account.

$$\frac{\sum_{i=1}^{n} l_i}{E_{\overline{CWS}}} = \sum_{i=1}^{n} \frac{l_i}{E_{i,CWS}} \tag{8}$$

The estimated regression coefficients, the standard deviation of the error term and their coefficients of variations are summarised in Tables 1 and 2. A comparison between the two regression models shows that $E_{\overline{CWS}}$ is in general about 700 MPa larger than $\overline{E}$. The differences between $E_{\overline{CWS}}$ and $\overline{E}$ are almost constant for all timber boards. However, with both models a large correlation coefficient $\rho \approx 0.96$ between the predicted and the measured stiffness properties is identified (Fig. 4a,b).

3.2 Model to predict the stiffness of knot sections

In the following, a model is developed in order to predict the tensile stiffness of each particular WS (E_{WS}).

Table 1 Parameters for the model to predict $E_{\overline{CWS}}$

	Expected value	COV	Correlation
β_0	8.52	0.0026	$\rho\ (\beta_0,\beta_1) = -9.54$
β_1	7.12×10^{-5}	0.023	$\rho(\beta_0, \sigma_\varepsilon) \approx 0$
σ_ε	5.47×10^{-2}	0.052	$\rho(\beta_1, \sigma_\varepsilon) \approx 0$

Table 2 Parameters for the model to predict $\overline{E}$

	Expected value	COV	Correlation
β_0	8.42	0.0021	$\rho\ (\beta_0,\beta_1) = -0.968$
β_1	7.41×10^{-5}	0.017	$\rho(\beta_0, \sigma_\varepsilon) \approx 0$
σ_ε	4.40×10^{-2}	0.052	$\rho(\beta_1, \sigma_\varepsilon) \approx 0$

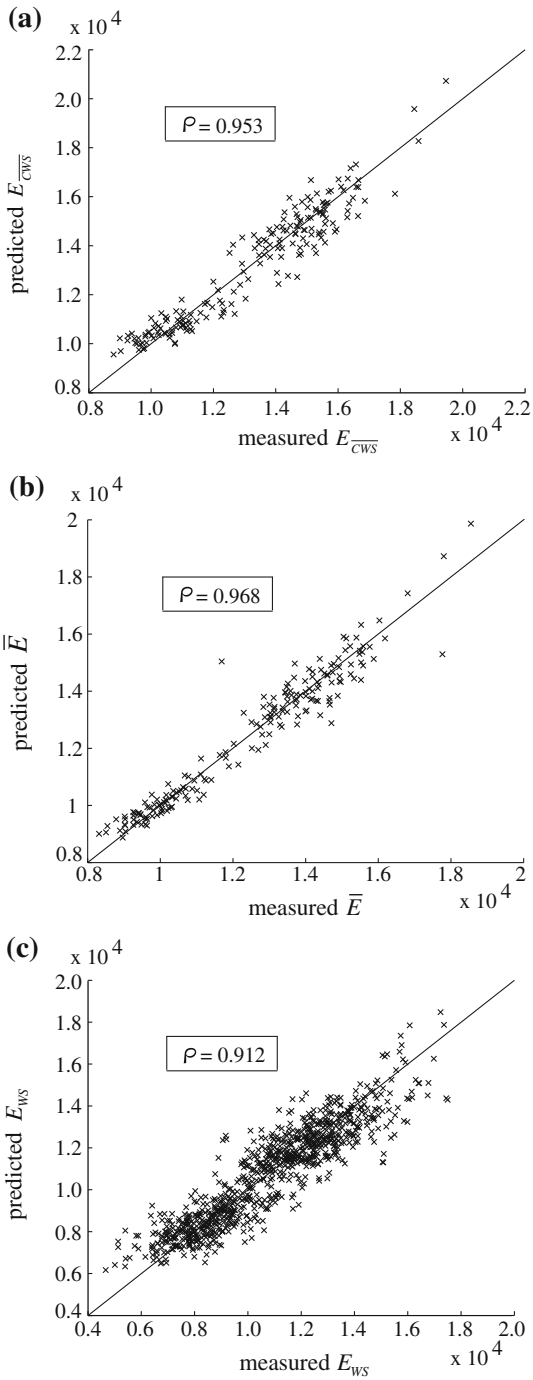

Fig. 4 Comparison between measured and predicted stiffness properties: **a** $E_{\overline{CWS}}$, **b** $\overline{E}$, and **c** E_{WS} (MPa)

Therefore, the measured stiffness properties of altogether 864 WS are taken into account. As described above, the model contains two parameters ($E_{\mathrm{dyn,F}}$ and tKAR). The estimated regression coefficients, the standard deviation of the error term and their coefficients of variations are summarised in Table 3. Using this model a rather large correlation $\rho = 0.912$ between the measured and the predicted stiffness can be identified (Fig. 4c).

Table 3 Parameter for the model to predict E_{WS}

	Expected value	COV	Correlation
β_0	8.41	0.0027	$\rho\ (\beta_0,\beta_1) = -0.922$
β_1	7.69×10^{-5}	0.019	$\rho\ (\beta_0,\beta_2) = -0.564$
β_2	-9.02×10^{-1}	0.040	$\rho\ (\beta_1,\beta_2) = 0.234$
σ_ε	1.00×10^{-1}	0.024	$\rho(\beta_i, \sigma_\varepsilon) \approx 0$

In order to control the outcome, a cross validation with four randomly selected sub-samples is performed (Hastie et al. 2001). Thereby, the model is developed based on three sub-samples and the results are validated using the fourth sub-sample. This is done four times for every sub-sample. The estimated model parameters are only slightly different and the correlation between the measured and the estimated stiffness properties are $0.90 < \rho < 0.92$.

The presented model is developed in order to predict the tensile strength of WS. If the model is used for the prediction of the stiffness of the CWS (using tKAR = 0) these are slightly underestimated. The difference of the measured and the predicted $E_{\overline{\text{CWS}}}$ is about 3 %. However, the measured and the predicted stiffness still show a large correlation $\rho = 0.953$. Thus, the model can also be applied to the prediction of the $E_{\overline{\text{CWS}}}$, when considering the underestimation.

In all the here described stiffness models, a very high correlation coefficient has been identified. This might be partly influenced by the investigated timber boards, which are two sub-samples of two different strength grades. However, the influence of the two sub-samples on the model parameters and the error term should be rather small as a result of the large variability of the measured stiffness properties within both strength grades.

4 Model to predict the tensile strength

In the following, two models for the prediction of the tensile strength are developed. The first one can be used for the prediction of the tensile capacity of the entire timber board f_t, whereas the second model can be used to predict the tensile strength of each particular knot cluster $f_{t,WS}$. For the estimation of both models the experimental results of the destructive tensile tests (Sample B) are used.

4.1 Model to predict the tensile strength of timber boards

The following model is developed in order to predict the tensile strength of the entire timber board. It is assumed that the tensile strength of the timber board corresponds to the tensile strength of the weakest section within the measured length. The weakest section is assumed to be the knot cluster having the largest tKAR-value. In order to ensure an optimal comparability to the stiffness model described above, the same parameters are chosen that are $E_{\text{dyn,F}}$ and tKAR. In Table 4 the estimated regression coefficients, the standard deviation of the error term and their coefficients of variations are summarised. Applying the model, a large correlation $\rho = 0.782$ between the estimated and the measured tensile capacities is identified (Fig. 5).

As known from several studies (e.g. Riberholt and Madsen 1979; Taylor and Bender 1991; Courchene et al. 1996; Isaksson 1999; Köhler 2006), the characteristics of the weakest section within a member is related to its length. With increasing length, the largest tKAR-value within a timber board (tKAR_{max}) increases and thus the tensile capacity decreases (size effect). Accordingly, the developed model can (without considering the size effect) only be used for the prediction of the tensile capacity of specimens having similar dimensions.

4.2 Model to predict the tensile strength of knot clusters

The second strength model is developed to predict the tensile strength of knot clusters or rather the tensile strength of WS. For the calculation, all WS within the measured area are considered; that includes a total number

Table 4 Parameter for the model to predict f_t

	Expected value	COV	Correlation
β_0	2.14	0.047	$\rho\ (\beta_0,\beta_1) = -0.944$
β_1	1.13×10^{-4}	0.059	$\rho\ (\beta_0,\beta_2) = -0.751$
β_2	-1.08	0.120	$\rho\ (\beta_1,\beta_2) = 0.520$
σ_ε	2.77×10^{-1}	0.034	$\rho(\beta_i, \sigma_\varepsilon) \approx 0$

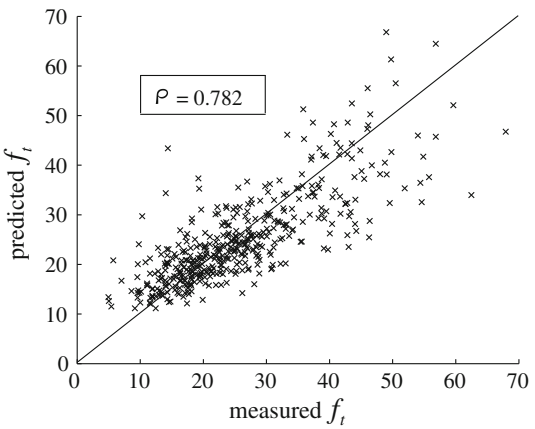

Fig. 5 Comparison between measured and predicted tensile capacity of timber boards f_t (MPa)

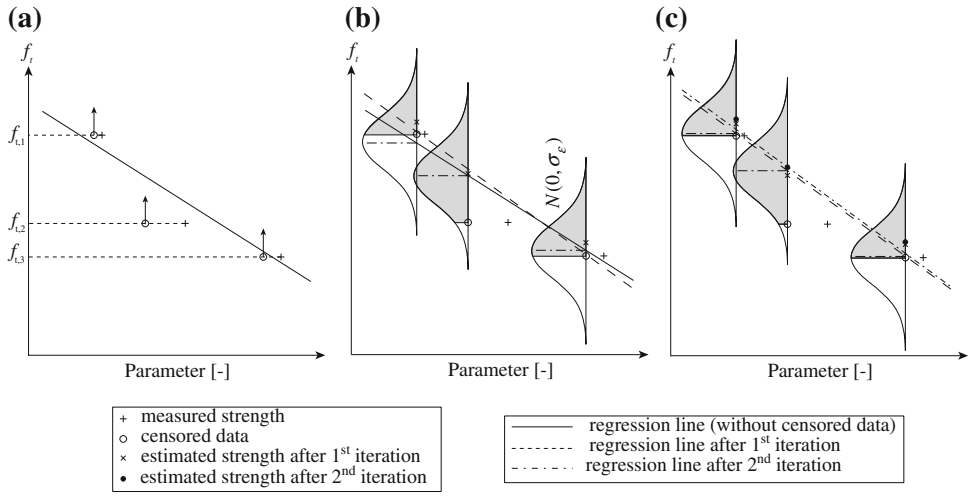

Fig. 6 Schematic illustration of the censored regression analysis

of 2,577 WS. As described above, a WS is defined as a section with tKAR $\geq$0.1. Based on the results of the destructive tensile tests, the tensile capacity of the timber boards and thus the tensile strength of the weakest section within each board are known. Further it is known that the tensile strength of all other WS is at least the tensile capacity of the corresponding timber board. In case of a timber board (three WS, tensile capacity of the entire board $f_t = 30$ MPa) the following information about the tensile strength of the WS can be obtained: Tensile strength of the weakest section $f_{t,WS} = 30$ MPa and tensile strength of the other two WS $f_{t,WS} \geq 30$ MPa.

With the given information it is possible to estimate the regression parameters by using linear regression analysis for censored data (see e.g. Buckley and James 1979; Catterjee and McLeich 1981). In Fig. 6, the principle of the regression analysis for censored data is illustrated. Figure 6a illustrates the measured tensile capacity $f_{t,i}$ of three timber boards (each timber board has two WS) and the corresponding parameter of each WS (e.g. tKAR-value). The weakest knot cluster within each member WS_+ is represented by '+' and the other knot cluster WS_o are represented by 'o'. Further, the illustration shows a linear regression line that describes the relation between the parameter of the weakest section and the corresponding tensile capacity. The regression curve and its corresponding σ_ε are calculated with Eq. (4)–(5). They are used as the start value for following calculations.

According to the principle of a linear regression model it is assumed that the error term ε is normal distributed around the regression model $\varepsilon \sim N(0, \sigma_\varepsilon)$. Based on this the strength of WS_o $f_{t,WS,o}$ can be estimated by the expected value of the truncated normal distribution (grey area) according to Eq. (9). Here, $f_{t,reg}$ denotes the expected tensile strength according to the regression model.

$$f_{t,WS,o} = \frac{\int_{f_{t,i}}^{\infty} x \cdot f(x)dx}{\int_{f_{t,i}}^{\infty} f(x)dx} \quad \text{with} \quad (9)$$

$$f(x) = \frac{1}{\sigma_\varepsilon \sqrt{2\pi}} \exp\left(-\frac{1}{2} \left(\frac{x - f_{t,reg}}{\sigma_\varepsilon} \right)^2 \right)$$

The estimated strength is illustrated with a 'x' (Fig. 6b). Using the estimated strength of WS_o and the measured strength of WS_+ a new regression model with a corresponding σ_ε can be calculated. The new regression line is illustrated as dashed line. With the new regression line and the corresponding σ_ε the strength of WS_o can be estimated again, following the principle described above. The new estimated strengths are illustrated as black dots in Fig. 6c. With the new estimated strength of WS_o and the measured strength of WS_+ a new regression model (dashed-dotted line) with a corresponding σ_ε can be estimated. This iteration has to be repeated up to the convergence criterion. In this study, a change between the estimated regression parameters in iteration step i and iteration step $i+1$ of 0.005 % is chosen. The estimated regression parameters of the strength model are summarised in Table 5. Furthermore, Fig. 7 illustrates the correlation between the measured/estimated tensile strength with the predicted tensile strength of all WS. It is obvious that the estimated tensile strength of the WS is located within the area near right of the regression model.

At this point, it has to be mentioned that this model is developed for the prediction of the tensile strength of WS. If the model is used for the prediction of the tensile strength of CWS (using tKAR = 0), it will be slightly underestimated. Further it has to be considered that the standard deviation of the estimated error term σ_ε will be underestimated using censored regression analysis. That results from

Table 5 Parameter for the model to predict $f_{t,WS}$

	Expected value	COV	Correlation
β_0	2.96	0.0067	$\rho\ (\beta_0,\beta_1) = -0.922$
β_1	8.50×10^{-5}	0.017	$\rho\ (\beta_0,\beta_2) = -0.596$
β_2	2.22	0.016	$\rho\ (\beta_1,\beta_2) = 0.274$
σ_ε	1.50×10^{-1}	0.014	$\rho(\beta_i, \sigma_\varepsilon) \approx 0$

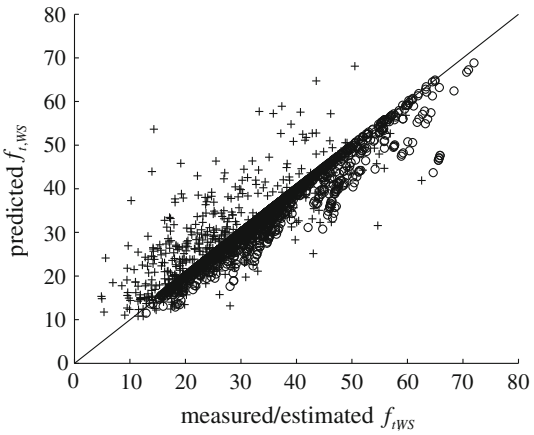

Fig. 7 Comparison between measured/estimated and predicted tensile strength of knot clusters $f_{t,WS}$

the fact, that the regression model is developed by using measured and estimated material properties and the latter ones are in general located nearby the regression line.

Another area of application of this model is the prediction of the tensile capacity of the entire timber board f_t. Therefore, the tensile capacity of one timber board $f_{t,i}$ is defined as the tensile strength of the weakest section within the board (j denotes the number of WS within the board i):

$$f_{t,i} = \min_j(f_{t,WS,ij}) \tag{10}$$

A comparison between the measured and the predicted tensile capacity shows a rather large correlation $\rho = 0.751$ (see the '+' within Fig. 7). An advantage of this method is that the tensile capacity of timber boards can be predicted independent of the board length.

4.3 Comparisons between the models

In the following, the two strength models described above are compared with each other. The significantly higher value of parameter β_0 within the second model indicates an higher predicted tensile strength within areas with small tKAR. On the other hand, the higher absolute value of parameter β_2 explains larger local strength reduction due to knots.

In Fig. 8, the estimated tensile strength of all WS (calculated with both models) are illustrated. Here '+' denotes the predicted tensile strength of the weakest section WS_+ and 'o' denotes the predicted strength of all other WS_o. It is obvious that the first strength model (model to predict f_t) underestimates the tensile strength of the majority of the WS. On average, the difference between the two models is $\Delta f_{t,WS} = 7.70$ MPa. However, the prediction of the tensile capacity of the timber boards f_t (which is assumed to be the tensile strength of the section with $tKAR_{max}$) is relatively similar, especially for timber boards with low resistance.

The difference between the two models can be explained by the following example: let's assume that a timber board with a tensile capacity $f_t = 30$ MPa contains a number of knot clusters. Let's assume further that the two largest knot clusters have the same tKAR-value (tKAR = 0.25). The first strength model is developed with the information about the tensile strength of one knot cluster with the specific tKAR-value; i.e. tKAR = 0.25 $\rightarrow f_{t,WS} = 30$ MPa. The second model is calibrated with the information that only one knot clusters with the specific tKAR-value will fail tKAR = 0.25 $\rightarrow f_{t,WS,1} = 30$ MPa, whereas the second knot cluster shows a higher tensile strength tKAR = 0.25 $\rightarrow f_{t,WS,2} \geq 30$ MPa.

5 Verification with existing models

In order to verify the introduced material model, it is compared with existing models. Therefore, the above mentioned material model presented in Blaß et al. (2008) will be used as a reference model. Between the two model approaches fundamental difference exists: (a) The test configuration between the studies is different. (b) Specimen size/testing length: The reference model is developed based on experimental investigations with specimen having a testing length of 137.5 mm; in the present study the testing length is >3,300 mm. (c) Measurement length: In the

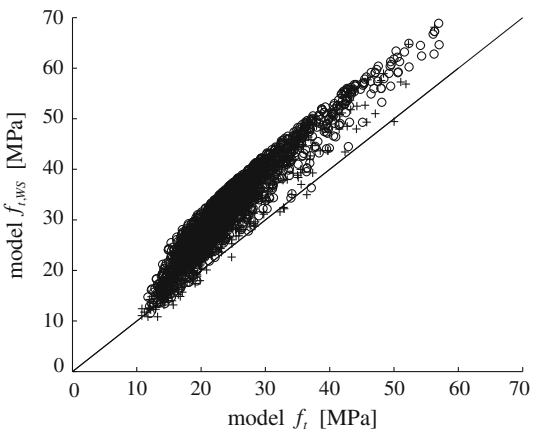

Fig. 8 Comparison between the strength models (MPa)

present study, the measurement length for measuring the stiffness properties varies depending on the natural growth characteristics of the investigated specimen. (d) Sample selection: The reference model is developed based on randomly selected timber board segments. Here a model is developed to predict E_{WS} and $f_{t,WS}$ – therefore only sections containing knot clusters are considered. (e) Input parameters: The reference model has used ρ_0 and tKAR, whereas in the present study the input parameters are $E_{\mathrm{dyn,F}}$ and tKAR. However, all the required input parameters are investigated on the timber boards presented in this study.

In the following, the stiffness properties $E_{\overline{CWS}}$ and E_{WS} as well as the tensile capacity of the timber boards f_t (tensile strength of the WS with tKAR_{max}) are estimated using both approaches. The results are illustrated in Fig. 9. In all illustrations an accordance between the estimated values (for both approaches) and the measured material properties exists within the upper part; i.e. timber boards or WS having relatively high strength and stiffness properties. However, within the lower part significant differences are detected. It is obvious that the here developed model shows good accordance—as it has been developed on the data-set itself. Nevertheless, all three illustrations indicate that the predictions using the reference model significantly overestimate the measured material properties, especially having low values of stiffness and strength. The overestimation is on average $\overline{\varepsilon}(E_{\overline{CWS}}) = 886$ MPa, $\overline{\varepsilon}(E_{WS}) = 374$ MPa and $\overline{\varepsilon}(f_t) = 9.80$ MPa.

The differences in Fig. 9a might be a result of the measurement length. Within the present study the tensile stiffness of the clear wood $E_{\overline{CWS}}$ is measured on the entire length between two adjacent knot clusters. Small defects between the knot clusters are not explicitly considered. Thus the measured stiffness might be lower as the stiffness of a defect-free specimen. However, it is still representing the mean stiffness properties of the clear wood sections.

It seems likely that the differences in Fig. 9b, c are resulting from the different dimensions of the test specimens. A drawback of small test specimens is that effects that are reducing the strength and stiffness properties, such as the influence of local grain deviation before and after the knot clusters are not considered. Further, lateral bending due to knots might be prevented. The influence is of particular importance for knot clusters having numerous knots and thus a large tKAR. Another reason for the differences might be the sample selection. As mentioned above, the emphasis of the present study is the investigation of the material properties of knot clusters and not of board sections. Thus, in particular sections containing knot clusters are considered.

For comparison of the tensile capacities, the different test setups have to be considered. When measuring the

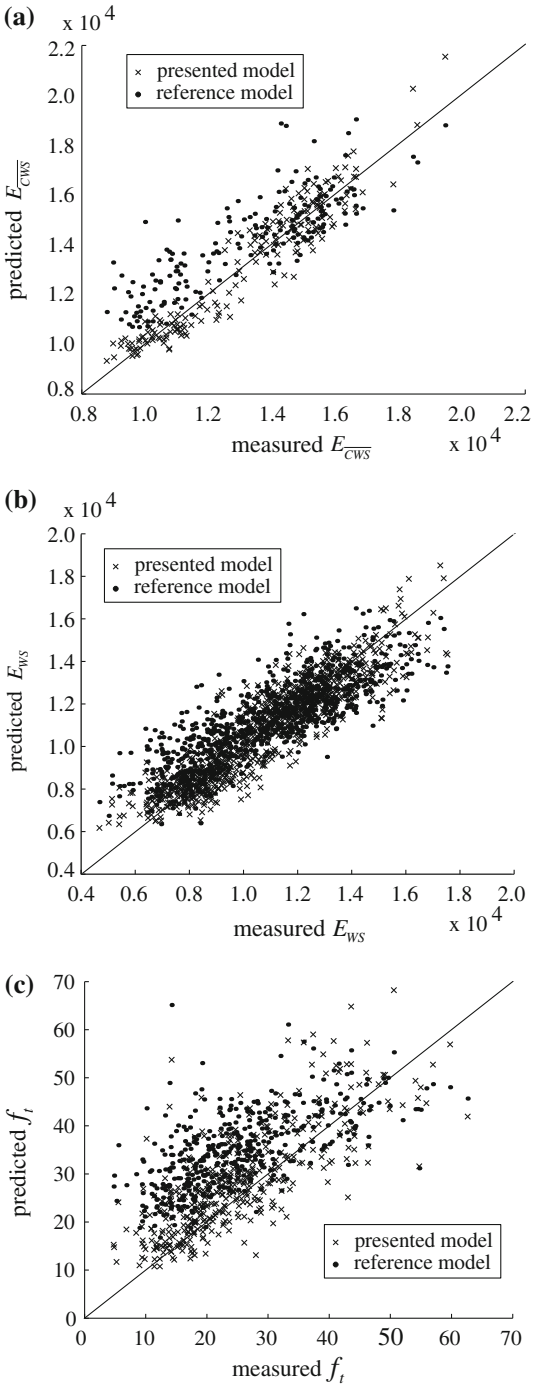

Fig. 9 Verification of the material models to predict **a** $E_{\overline{CWS}}$, **b** E_{WS}, and **c** E_t (MPa)

tensile strength using the test configuration described in Heimeshoff and Glos (1980), the investigated timber boards are supported through glued timber boards within the transition area. Thus, knot clusters, where parts of the fracture are outside the testing length (137.5 mm), are reinforced. The influence might be significant as a result

that by the majority of the investigated timber boards, the area of the fracture is above 137.5 mm.

6 Modelling of the material properties

With the stiffness and strength models described above it is possible to model the material properties (tensile stiffness and tensile strength) over the entire board. Therefore, only information about the $E_{\mathrm{dyn,F}}$ and the tKAR-value is necessary.

In the following the material properties of a timber board will be predicted based on the measured values given in Table 6. The tensile stiffness and the tensile strength are predicted with the models E_{WS} and $f_{\mathrm{t},WS}$. As described above, the tensile stiffness and the tensile strength of the clear wood will be slightly underestimated with this model. Thus in this example, both the estimated tensile stiffness and the estimated tensile strength of the clear wood are increased by 3 %. The results are illustrated in Table 7 and Fig. 10.

Table 6 Example: input parameter

	WS_1	WS_2	WS_3	WS_4	WS_5
$E_{\mathrm{dyn,F}}$ (MPa)			12,000		
tKAR (-)	0.30	0.25	0.50	0.31	0.23
Position (mm)	600	1,400	1,900	2,700	3,600

Table 7 Example: estimated tensile strength and tensile stiffness

	CWS	WS_1	WS_2	WS_3	WS_4	WS_5
E_t (MPa)	11,691	8,660	9,060	7,231	8,583	9,225
f_t (MPa)	54.9	27.4	30.6	17.6	26.8	32.0

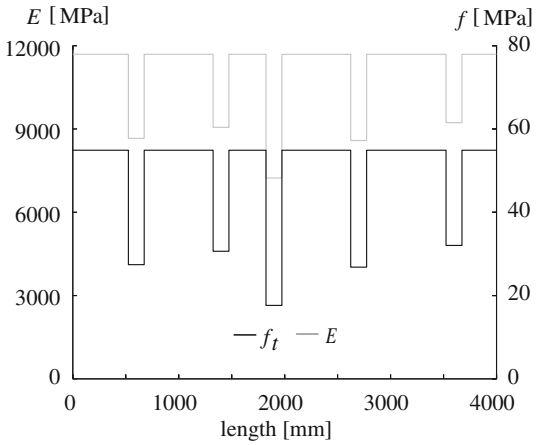

Fig. 10 Example: estimated tensile strength and tensile stiffness

7 Conclusion

In the present paper, a model for the prediction of the local strength and stiffness properties is developed. The specific characteristic of these models is that material properties are described according to their morphological characteristics; i.e. the boards are subdivided into sections containing knots (knot sections) and sections without knots (clear wood sections). From those sections, the material properties are estimated based on results of destructive and non-destructive tensile tests.

The experimental investigation takes place on a total of 650 timber boards. From all boards, the dynamic modulus of elasticity based on Eigenfrequency measurement is estimated. Further, the dimension and position of all knots with a diameter larger than 10 mm are documented. Based on them the tKAR-value over the entire length of the timber boards is calculated. On 200 of the timber boards, non-destructive tensile tests are performed. Before testing, the timber boards are subdivided into knot sections and clear wood sections. From each section, the strains are measured using an optical camera device. Based on this, the corresponding stiffness is estimated. On the other 450 timber boards, destructive tensile tests are performed to estimate the tensile capacity.

Based on the results, a model for the prediction of the tensile stiffness is developed. The model can be used for the prediction of the stiffness of each particular knot section and for the prediction of the clear wood. For both, large correlations between the measured and the predicted stiffness properties are identified, $\rho = 0.912$ and $\rho = 0.953$, respectively.

Furthermore, a model for the prediction of the tensile strength of each particular knot section is developed. The parameters of the model are estimated using censored regression analysis. Within this method, information on the failed knot section and information on the other knot sections (within the timber board) are considered. The model can be used for the prediction of the tensile capacity of the entire timber board. Therefore, it has to be assumed that the tensile capacity of the entire timber board corresponds to the tensile capacity of the weakest knot section within the board. The analysis of the model shows a correlation $\rho = 0.751$ between the measured and the predicted tensile capacity. An advantage of this method is that the tensile capacity of timber boards can be predicted independent of their geometric shape.

With the here developed material models it is possible to predict the strength and stiffness properties over the entire timber board based on information about $E_{\mathrm{dyn,F}}$ and tKAR. Such a model can be used for the development of more efficient grading criteria. Furthermore, it can be applied to modelling of the material properties within timber products, such as glulam.

References

Benjamin JR, Cornell CA (1970) Probability, statistics and decisions in civil engineering. Mc Graw-Hill Book Company, New York

Blaß HJ, Frese M, Glos P, Denzler JK, Linenmann P, Ranta-Maunus A (2008) Zuverlässigkeit von Fichten-Brettschichtholz mit modifiziertem Aufbau, vol 11. KIT Scientific Publishing, Karlsruhe

Boatright SWJ, Garrett GG (1979a) The effect of knots on the fracture strength of wood i. a review of methods of assessment. Holzforschung 33(3):68–72

Boatright SWJ, Garrett GG (1979b) The effect of knots on the fracture strength of wood ii. a comparative study of methods of assessment, and comments on the application of fracture mechanics to structural timber. Holzforschung 33(3):72–77

Buckley J, James I (1979) Linear regression with censored data. Biometrika 66:429–36

CEN (2003) DIN EN 408, Timber structures, structural timber and glued laminated timber, determination of some physical and mechanical properties. German version

CEN (2009) DIN EN 14081-4, Timber structures, strength graded structural timber with rectangular crosssection Part 4: Machine grading Grading machine settings for machine controlled systems. German version

CEN (2010) DIN EN 384, Structural timber, Determination of characteristic values of mechanical properties and density. German version EN 384:2010

Chatterjee S, McLeich DL (1981) Fitting linear regression models to censored data by least squares and the method of maximum likelihood. Tech. rep., Department of statistics, Standford University

Courchene T, Lam F, Barrett J (1996) The effects of edge knots on the strength of spf msr lumber. In: Proceedings of the 29th Meeting, International Council for Research and Innovation in Building and Construction, Working Commission W18,Timber Structures, Bordeaux, France, CIB-W18, Paper No. 29-5-1

Denzler JK (2007) Modellierung des Grösseneffektes bei biegebeanspruchtem Fichtenschnittholz. PhD thesis, TU München

Ehlbeck J, Colling F, Görlacher R (1985) Einfluß keilgezinkter Lamellen auf die Biegefestigkeit von Brettschichtholzträgern Eingangsdaten für das Rechenmodel. Eur J Wood Prod 43(8):369–373

Faber M (2012) Statistics and probability theory: in pursuit of engineering decision support, vol 18. Springer, Berlin Heidelberg

Fewell A (1982) Machine stress grading of timber in the united kingdom. Holz Roh- Werkst 40(12):455–459

Fink G, Kohler J (2011) Multiscale variability of stiffness properties of timber boards. In: ICASP Applications of Statistics and Probability in Civil Engineering. Zurich, Switzerland

Fink G, Kohler J (2012) Zerstörungsfreie Versuche zur Ermittlung des Elastizitätsmodules von Holzbrettern. IBK Report No. 339, ETH Zürich, Zurich

Fink G, Deublein M, Kohler J (2011) Assessment of different knot-indicators to predict strength and stiffness properties of timber boards. In: Proceedings of the 44th Meeting, International Council for Research and Innovation in Building and Construction, Working Commission W18, Timber Structures, Alghero, Italy, CIB-W18, Paper No. 44-5-1

Giudiceandrea F (2005) Stress grading lumber by a combination of vibration stress waves and x-ray scanning. In: Proceedings of the 11th International Conference on Scanning Technology and Process optimization in the wood Industry (ScanTech 2005)., Las Veagas

Glos P (1978) Zur Bestimmung des Festigkeitsverhaltens von Brettschichtholz bei Druckbeanspruchung aus Werkstoff- und Einwirkungskenngrößen. Sonderforschungsbereich 96, Techn. Univ

Görlacher R (1990) Sortierung von Brettschichtholzlamellen nach DIN 4074 durch Messung von Longitudinalschwingungen. Bauingenieur 65:517–522

Görlacher (1984) Ein neues Messverfahren zur Bestimmung des Elastizitätsmoduls von Holz. Holz Roh- Werkst 42:219–222

Hastie T, Tibshirani R, Friedman J (2001) The elements of statistical learning, vol 1. Springer, Berlin Heidelberg

Heimeshoff B, Glos P (1980) Zugfestigkeit und Biege-E-Modul von Fichten-Brettlamellen. Eur J Wood Prod 38(2):51–59

Isaksson T (1999) Modelling the variability of bending strength in structural timber. PhD thesis, Lund Institute of Technology

Kline D, Woeste F, Bendtsen B (1986) Stochastic model for modulus of elasticity of lumber. Wood Fiber Sci 18:228–238

Köhler J (2006) Reliability of timber structures. Phd, ETH Zurich, reliability/Probability Theory

Köhler J, Sørensen JD, Faber MH (2007) Probabilistic modeling of timber structures. Struct saf 29(4):255–267

Kohler J, Brandner R, Thiel A, Schickhofer G (2013) Probabilistic characterisation of the length effect for parallel to the grain tensile strength of central european spruce. Eng Struct 56:691–697

Kollmann F, Krech H (1960) Dynamische Messung der elastischen Holzeigenschaften und der Dämpfung ein Beitrag zur zerstörungsfreien Werkstoffprüfung. Holz Roh- Werkst 18(2):41–54

Mitsuhashi K, Poussa M, Puttonen J (2008) Method for predicting tension capacity of sawn timber considering slope of grain around knots. J Wood Sci 54(3):189–195

Riberholt H, Madsen PH (1979) Strength of timber structures, measured variation of the cross sectional strength af structural lumber. Tech. rep., Struct. Research Lab., Technical University of Denmark

Samson M, Blanchet L (1992) Effect of knots on the flatwise bending stiffness of lumber members. Eur J Wood Prod 50(4):148–152

Sandomeer MK, Köhler J, Faber MH (2008) Probabilistic output control for structural timber, modelling approach. In: Proceedings of the 41th Meeting, International Council for Research and Innovation in Building and Construction, Working Commission W18 - Timber Structures, St. Andrews, Canada, CIB-W18, Paper No. 41-5-1

Steiger R (1996) Mechanische Eigenschaften von Schweizer Fichten-Bauholz bei Biege-, Zug-, Druck und kombinierter M/N-Beanspruchung-Sortierung von Rund- und Schnittholz mittels Ultraschall. PhD thesis, ETH Zurich

Taylor SE, Bender DA (1991) Stochastic model for localized tensile strength and modulus of elasticity in lumber. Wood Fiber Sci 23 (Number 4):501–519